NASA CR-
159997

Erwin Hirschmann,
Code 727

APL/JHU
SIR78U-039
August 1978

CUMULATIVE SLANT PATH RAIN ATTENUATION STATISTICS ASSOCIATED WITH THE COMSTAR BEACON AT 28.56 GHz FOR WALLOPS ISLAND, VIRGINIA

by JULIUS GOLDHIRSH

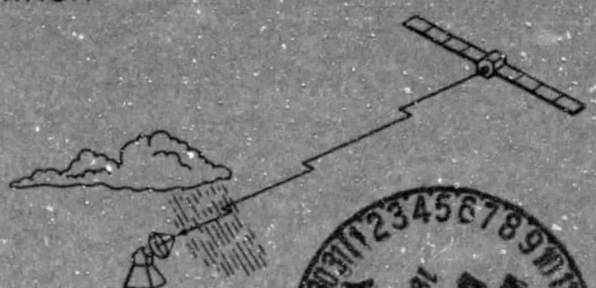

SPACE DEPARTMENT
THE JOHNS HOPKINS UNIVERSITY ■ APPLIED PHYSICS LABORATORY

APL/JHU
SIR78U-039
August 1978

CUMULATIVE SLANT PATH RAIN ATTENUATION STATISTICS ASSOCIATED WITH THE COMSTAR BEACON AT 28.56 GHz FOR WALLOPS ISLAND, VIRGINIA

by JULIUS GOLDHIRSH

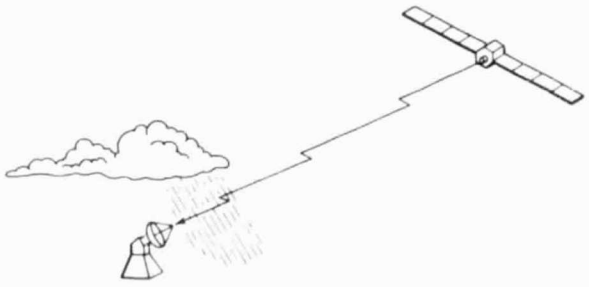

SPACE DEPARTMENT
THE JOHNS HOPKINS UNIVERSITY ■ APPLIED PHYSICS LABORATORY
Johns Hopkins Road, Laurel, Maryland 20810

Operating under Contract N00024-78-C-5384 with the Department of the Navy

THE JOHNS HOPKINS UNIVERSITY
APPLIED PHYSICS LABORATORY
LAUREL MARYLAND

CUMULATIVE SLANT PATH RAIN ATTENUATION STATISTICS ASSOCIATED WITH THE COMSTAR BEACON AT 28.56 GHz FOR WALLOPS ISLAND, VIRGINIA

Julius Goldhirsh

Applied Physics Laboratory
The Johns Hopkins University
Laurel, Maryland

ABSTRACT

Cumulative slant path rain attenuation statistics at 28.56 GHz are given for the year period 1 April 1977 through 31 March 1978 for Wallops Island, Virginia. These results were arrived at using direct measurements of a beacon signal emanating from the COMSTAR geosynchronous satellite. Yearly, monthly, and time of day fade statistics are presented and characterized. In addition, a 19.04 GHz yearly fade distribution, corresponding to a second COMSTAR beacon frequency, is predicted using the concept of effective path length, disdrometer, and rain rate results.

Specifically, it is shown that the yearly attenuation and rain rate distributions follow with good approximation log normal variations for most fade and rain rate levels, respectively. Attenuations were exceeded for the longest and shortest periods of times for all fades in August and February, respectively. These months thus represented the "worst" and "best" months at all attenuation levels. The eight hour time period showing the maximum and minimum number of minutes over the year for which fades exceeded 12 dB were approximately between 1600 to 2400, and 0400 to 1200 hours (local time), respectively.

In employing the predictive method for obtaining the 19.04 GHz fade distribution, it is demonstrated theoretically that the ratio of attenuations at two frequencies is minimally dependent on raindrop size distribution providing these frequencies are not widely separated (such as 28 and 19 GHz).

THE JOHNS HOPKINS UNIVERSITY
APPLIED PHYSICS LABORATORY
LAUREL MARYLAND

CUMULATIVE SLANT PATH RAIN ATTENUATION STATISTICS ASSOCIATED WITH THE COMSTAR BEACON AT 28.56 GHz FOR WALLOPS ISLAND, VIRGINIA

1.0 INTRODUCTION

The need to amass long term slant path fade statistics for various geographic locations in the U.S. at frequencies above 10 GHz resulted in the stationing of the COMSTAR satellites in geosynchronous orbits [1]. These satellites which have beacons at 19.05 and 28.56 GHz were built by Hughes Aircraft, are owned and controlled in orbit by COMSAT General Corporation, and are leased to AT&T and GT&E Companies for domestic U.S. communication service.

In the design of high frequency earth-satellite communication systems, it is desirable to have a knowledge of the attenuation distribution or the expected percentage of the time the attenuation due to rain exceeds certain levels. Such information may be used in establishing transmitter power margins and receiver sensitivity requirements. In addition, it is desirable that the designer be equipped with a knowledge of monthly as well as time of day fade statistics. Using this information, for example, transmitter power margins can be temporarily adjusted to handle the increased fades during certain months of the year or periods of time during the day.

From 1 April 1977 to 31 March 1978, the COMSTAR beacon signal at 28.56 GHz has been received continuously at Wallops Island, Virginia (located 180 km southeast of Washington, D. C., off the mid-Atlantic coast). During periods of rain the signal is monitored down to approximately 30 dB below the free space level and these data are digitized and recorded on tape for later reduction and analysis. Ancillary measurements such as rain drop size distributions and rain rates are also obtained continuously with nearby disdrometers and raingages, respectively. In addition, a high resolution, S-band radar monitors the rain reflectivity along the earth-satellite path during selected periods of rain.

Employing the 1977 summer data base, it has been demonstrated previously that radar and disdrometer measurements enable the prediction of

individual fade events and long term distributions with good accuracy [2,3,4]. In this report we present and characterize the cumulative fade statistics for the 1977-78 year period. Also presented are the month and time of day statistics as well as the raingage rain rate distribution. The concept of effective path length using the 28.56 GHz fade and measured rain rate distribution are employed to predict the 19.04 GHz fade distribution. Predicted distributions for the year period are arrived at from disdrometer data, radar results [2,4], as well as from the distributions of Bergmann [5] obtained using the 28 and 19 GHz COMSTAR beacons.

2.0 EXPERIMENTAL CONFIGURATION

As the details of the radar and receiver experimental configuration have been presented previously, we give here only a brief description.

The experimental configuration consists of a phase locked loop receiving system operating at 28.56 GHz, an S-band radar (f = 2.84 GHz) located approximately 30 m away, and a system of three raingages and two disdrometers located in the immediate vicinity of the receiving antenna. Both antennas are fixed and point in the direction of the COMSTAR geosynchronous satellite (95°W longitude $\pm$ 0.1°) with elevation and azimuth angles of 41.6° and 210°, respectively.

The pertinent parameters for the COMSTAR receiving system are given in Table 1.

3.0 CUMULATIVE FADE STATISTICS

In this section we describe the yearly, monthly, and time of day cumulative fade statistics for Wallops Island, Virginia, region as measured at 28.56 GHz for the period 1 April 1977 through 31 March 1978. These data were originally recorded on tape and later reduced and analyze using an HP 9825 minicomputer.

3.1 Year Fade Distribution

In Figure 1 is plotted on a semi-log scale the overall measured 28.56 GHz exceedance probability as a function of ~~rain rate~~ fade depth. These results constitute the fade statistics for 82 rain days during the year period.

Table 1

PERTINENT COMSTAR RECEIVING SYSTEM PARAMETERS

Antenna Gain	52.7 dB
Beamwidth	0.4°
Antenna Diameter	1.83 m (6 ft)
Free Space Power Received	-106 dBm
ERP	55.8 dBm
Path Loss	-213.4 dB
Line Loss	-0.5 dB
Sky Loss	-0.3 dB
Phaselock Hold-in Threshold	-138 dBm
Phaselock Acquisition Threshold	-133 dBm
Dynamic Range (minimum)	32 dB
Predetection 3 dB Bandwidth	50-100 Hz
Post Detection 1 dB Bandwidth	10-20 Hz
Amplitude Measurement Error	$\pm$ 1 dB
Noise Figure	18 dB

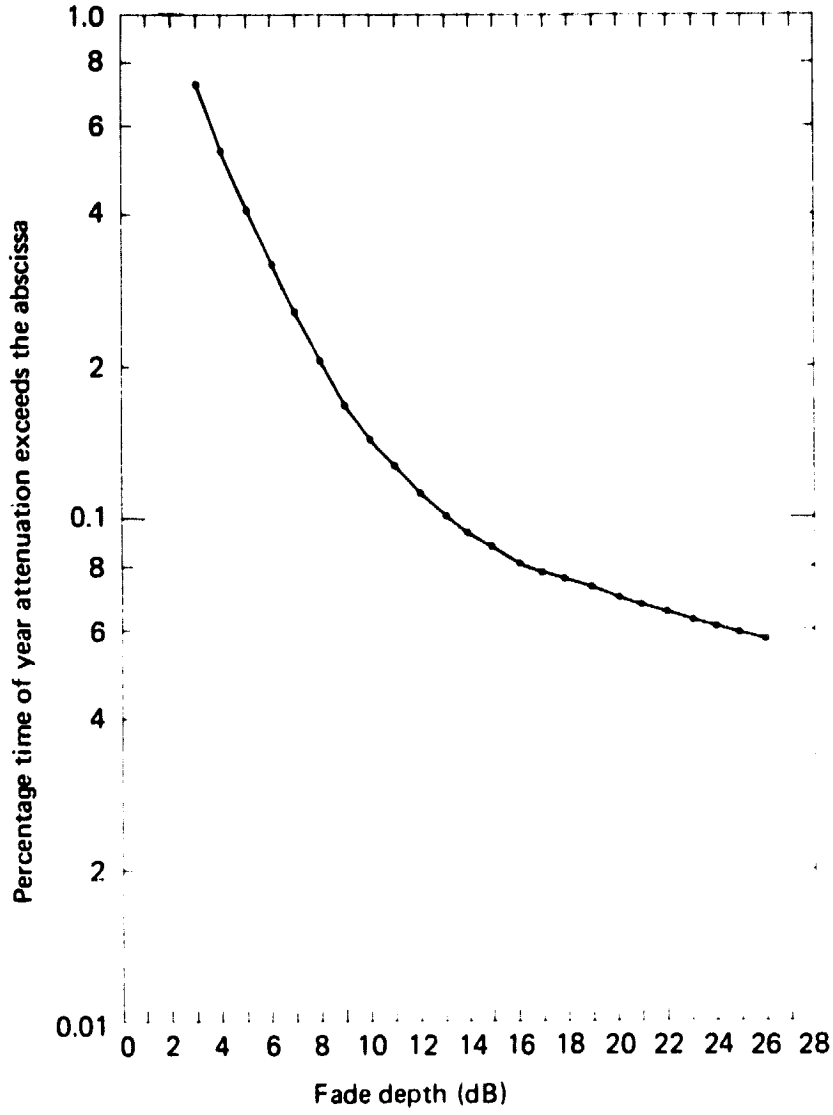

Figure 1. Cumulative slant path fade distribution at 28.56 GHz for the year period 1 April 1977 to 31 March 1978, plotted on a semi-logarithmic scale.

During this interval, the receiver operated continuously with negligible down time. The times for which the fades exceeded 3 and 25 dB were 3814 and 312 minutes, respectively.

In Figure 2 the same distribution is plotted on a log-normal scale and we note that an excellent fit exists down to about 17 dB. The deviation from log normal at higher fades may be due to an insufficient data base. This result is consistent with the contention of Lin [6] that long term distributions should follow a log normal variation; a notion not universally accepted. It is interesting to note that the year period rain rate distribution also follows with good approximation the log normal distribution over most of the rain rate intervals (Fig. 13).

3.2 Monthly Statistics

In Figures 3 through 5 are plotted the individual monthly distributions for the given year period where the ordinate represents the percentage of the month the attenuation exceeds the abscissa value. We note that for all fades, August and June represent the "worst" and "next worst" months, respectively, and February was the "best" month during which fading times were minimum. In Figure 6 we summarize these results in the form of histograms; the ordinate representing the percentage of the month the fade exceeds 5 (white), 15 (black), and 25 (grey) dB and the abscissa represents the month of the year. We note that in August, fades of 5, 15, and 25 dB were exceeded 393, 132, and 98 minutes, respectively.

The above results are consistent with the long term monthly rainfall measurements presented in Figure 7 and taken by the U.S. Navy and U.S. Weather Service for the Wallops Station. The ordinate represents the total number of millimeters of rainfall and the abscissa is the month of the year. The monthly averages are taken over a period of 25 to 28 years and are denoted by the center horizontal lines. Also indicated are the plus and minus standard deviations taken about the respective average. The rainfall amount for the individual months of the 1977-78 year period are also given (solid dots). We note that the August rainfall was well above the average plus its standard deviation and June was well above its

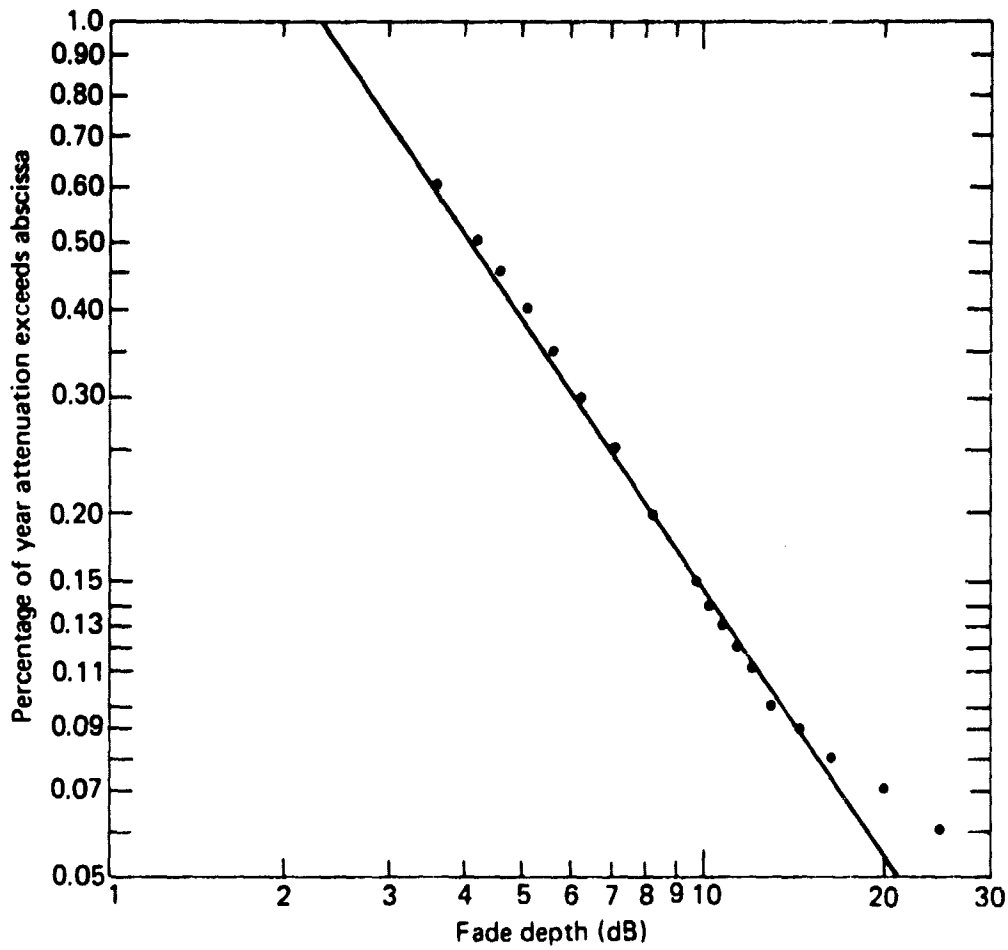

Figure 2. Cumulative slant path fade distribution at 28.56 GHz for the year period 1 April 1977 to 31 March 1978, plotted on a log-normal scale.

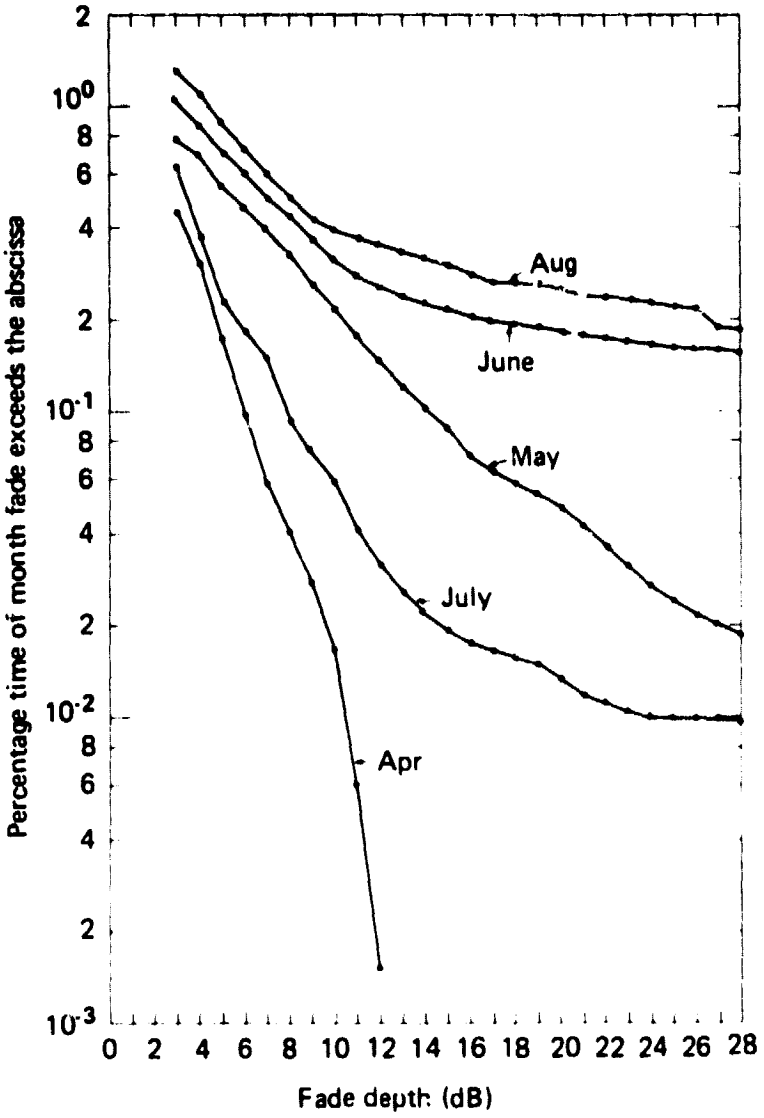

Figure 3. Cumulative fade distributions for the indicated months during the year period 1 April 1977 through 31 March 1978.

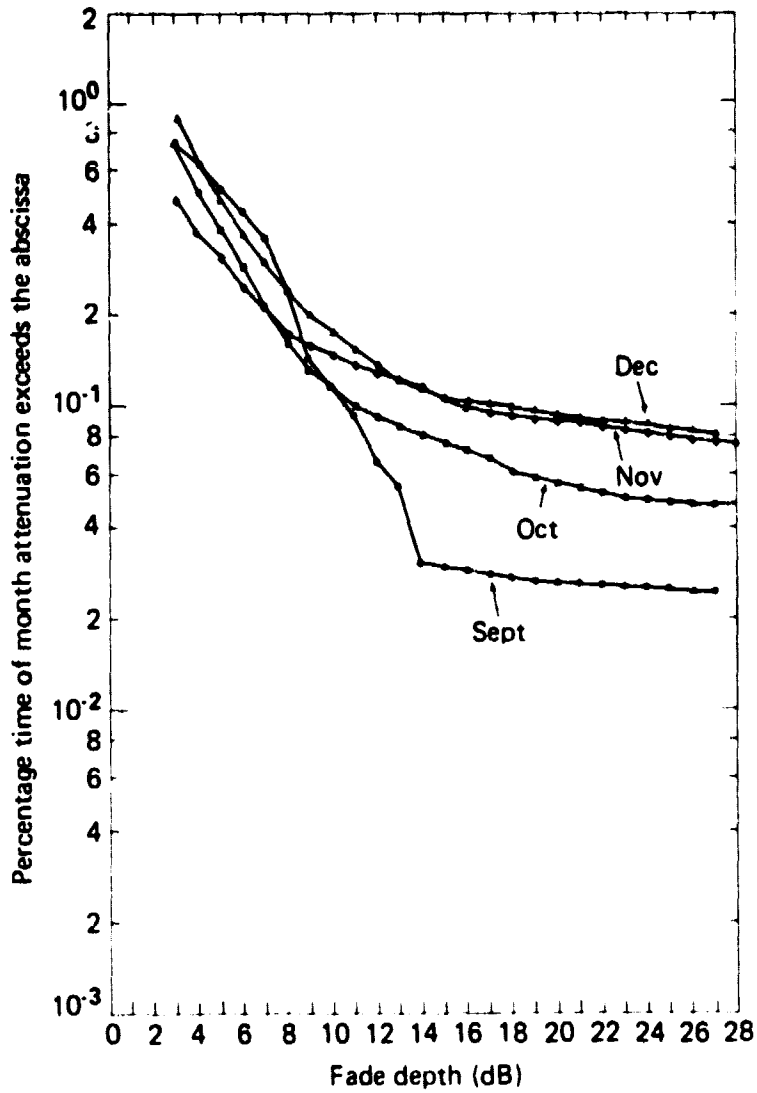

Figure 4. Cumulative fade distributions for the indicated months during the year period 1 April 1977 through 31 March 1978.

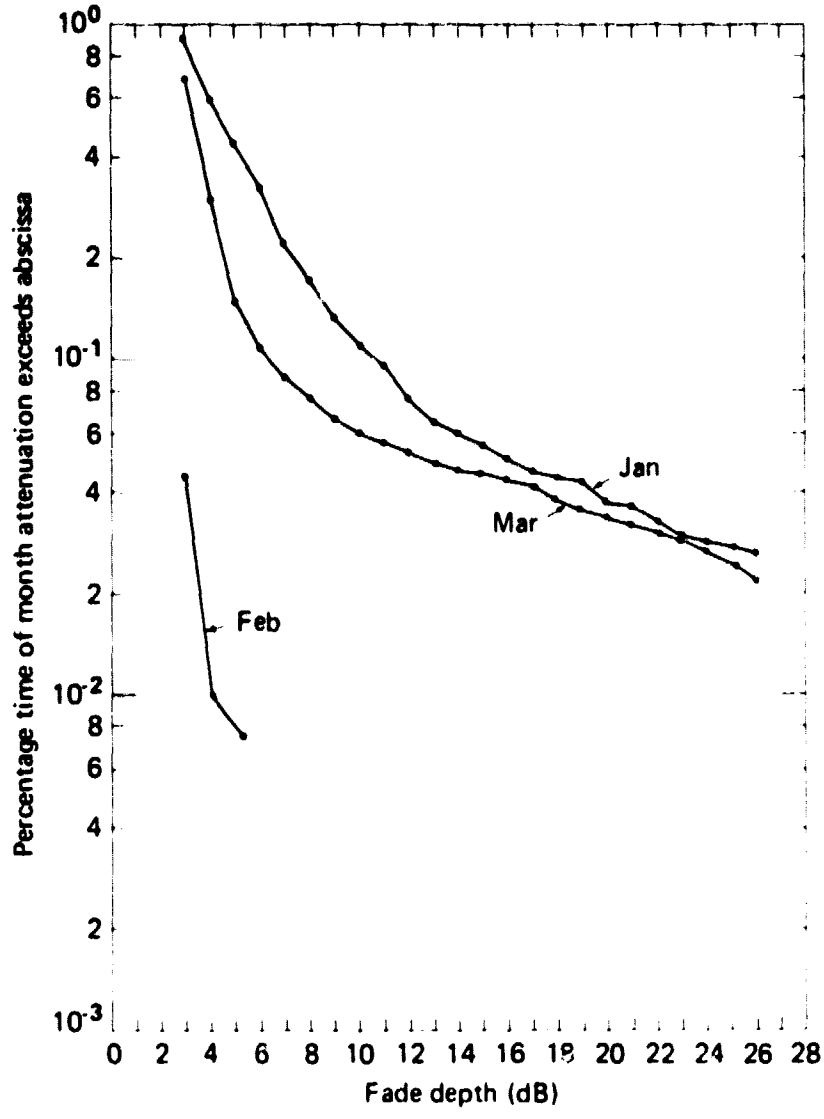

Figure 5. Cumulative fade distributions for the indicated months during the year period 1 April 1977 through 31 March 1978.

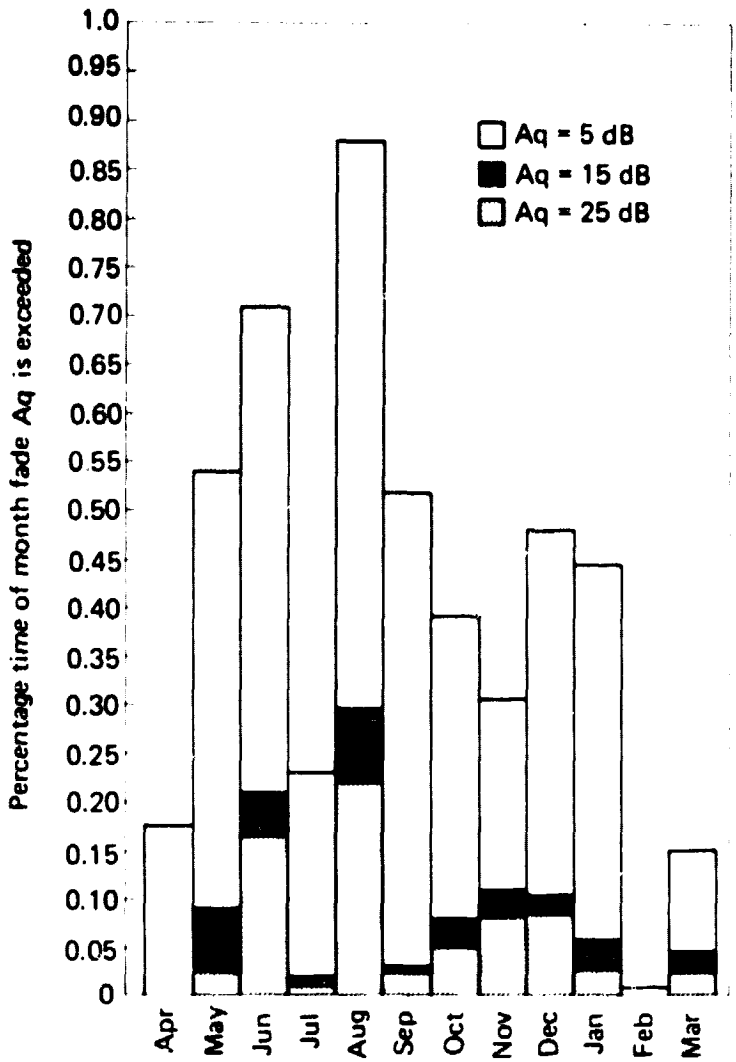

Figure 6. Histogram denoting the percentage times for the various months the fades of 5 (white), 15 (black), and 25 (grey) dB are exceeded.

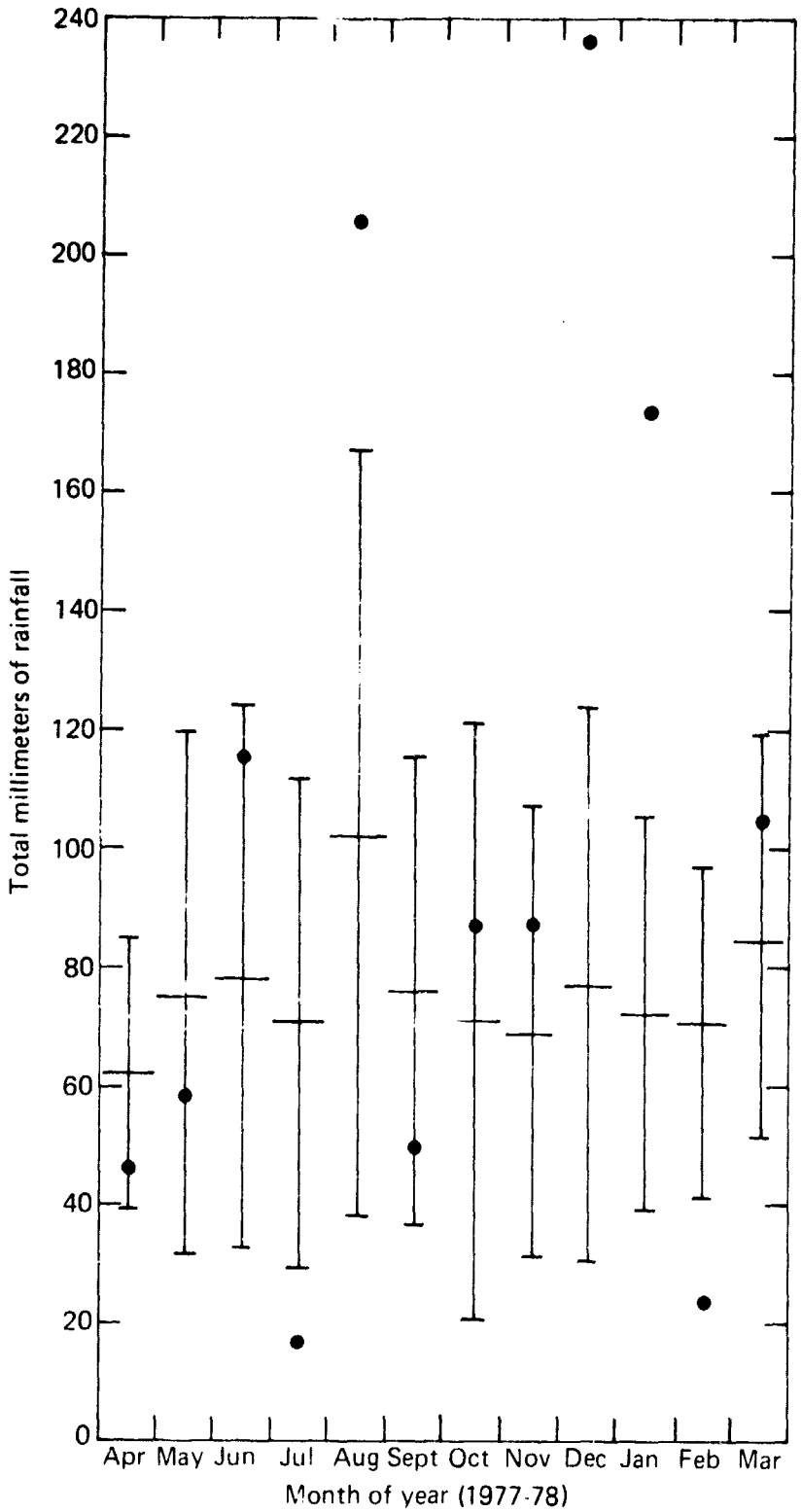

Figure 7. The average monthly rainfall in millimeters (center horizontal lines) for Wallops Island, Virginia, taken over a 25 to 28 year period. Also shown are the plus and minus standard deviations (vertical extensions about the average) as well as the 1977-78 monthly rainfall (solid dots).

average. On the other hand, February was well below its average minus its standard deviation. Specifically, in August and June of 1977 there were 205 and 116 mm of rainfall as compared to the respective monthly averages of 102 and 78 mm. For February of 1978 the precipitation measured 24 mm as compared to the monthly average of 69 mm.

It is interesting to note from Figure 7 that August represents the "worst" month from the rainfall standpoint (highest average monthly rainfall) and this is identical to the worst month from the fade statistic standpoint for the 1977-78 period. This agreement suggests the possibility of using long term average monthly rainfall data as an indicator of the worst month for the higher fades.

For seven months of the year, the rainfall amounts were within the long term monthly averages plus and minus the respective standard deviations and for five months the monthly rainfalls were outside these ranges. Based on these results, we note that the overall monthly rainfall values measured for the 1977-78 period are not representative of those for the long term average year.

3.3 Worst Month Statistics

The curves given in Figure 8 characterize the worst months fades relative to the yearly fade. The upper curve describes the ratio of the monthly to the year exceedance probabilities (left hand scale). This ratio has been characterized by Crane and Debrunner [7] for the case in which the denominator corresponds to a multiyear data base. This quantity is bounded between 1 and 12 for a 1 year return period; the lower bound representing the case where the number of minutes the fades were exceeded for each month of the year are the same and the upper bound corresponds to the case where fades are only experienced during the worst month. Crane and Debrunner have demonstrated that if an exponential distribution is applied to the expected occurrence of the monthly probabilities, the ratio should be less than 4.4. We note from Figure 8 that the ratio for the year period is smaller or equal to 3.74 over the given fade range.

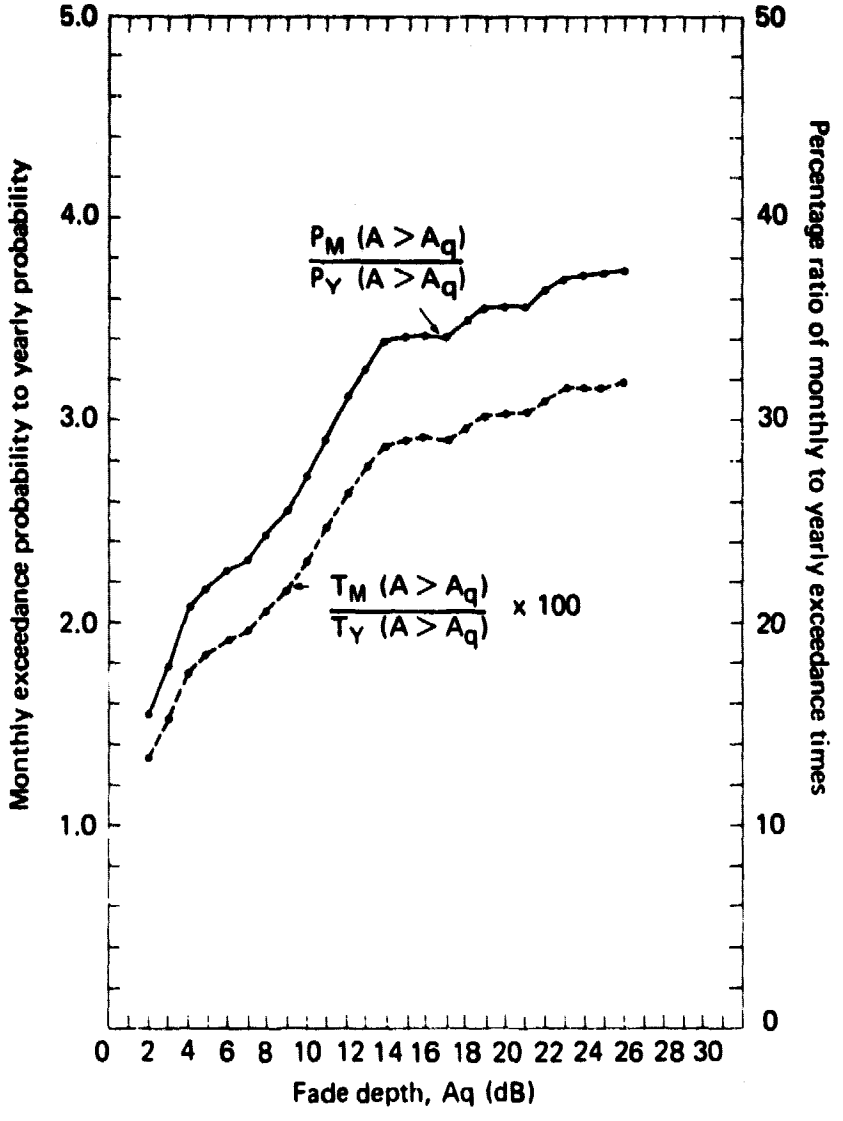

Figure 8. Monthly to yearly exceedance probability (upper curve-left hand scale) as a function of fade depth. Also plotted is the percentage monthly to yearly exceedance times (right hand scale).

The lower curve in Figure 8 gives the percentage ratio of the monthly to the yearly times for which the abscissa fades are exceeded. For example, of the 25 dB or greater fades that occurred during the entire year we note that 31% of these occurred in August.

3.4 Time of Day Statistics

In order to establish the periods during the day in which earth-satellite communications may be most and least influenced by rain attenuation, we present the fade distributions and histograms depicted in Figures 9 and 10. In these figures are given the percentage of the time of the year various fade depths are exceeded during six four-hour periods of the day. We note that the six distributions in Figure 9 tend to group into three distinct pairs for fades exceeding 12 dB. Two of these groupings represent eight contiguous hours each. We note, for example, that between the hours of 2000 to 0400 GMT (approximately 1600 to 2400 local time) the number of minutes for which fades of 12 dB or more are exceeded are greater than during any other period. The eight-hour period showing the minimum number of minutes is between 0800 to 1600 GMT (approximately 0400 to 1200 local time). These two eight-hour periods of time most likely represent the periods of maximum and minimum convection, respectively, caused by ground heating.

4.0 PREDICTION OF THE 19.04 GHz FADE

In this section we describe the method by which the 19.04 GHz fades may be predicted. This method uses the concept of effective path length applied to measured fade and rain rate distributions and has been successfully employed using the 1977 summer data base [2,4].

4.1 Predicted and Measured Ratio of Fades

Describing this technique in a somewhat different fashion, we assume that a cumulative rain rate and fade distribution at frequency, f_1, have been measured, and it is desired to establish the fade distribution at frequency, f_2. We initially define attenuations A_{i1} and A_{i2} as the respective frequencies, f_1 and f_2, for a given exceedance probability, P_i, by,

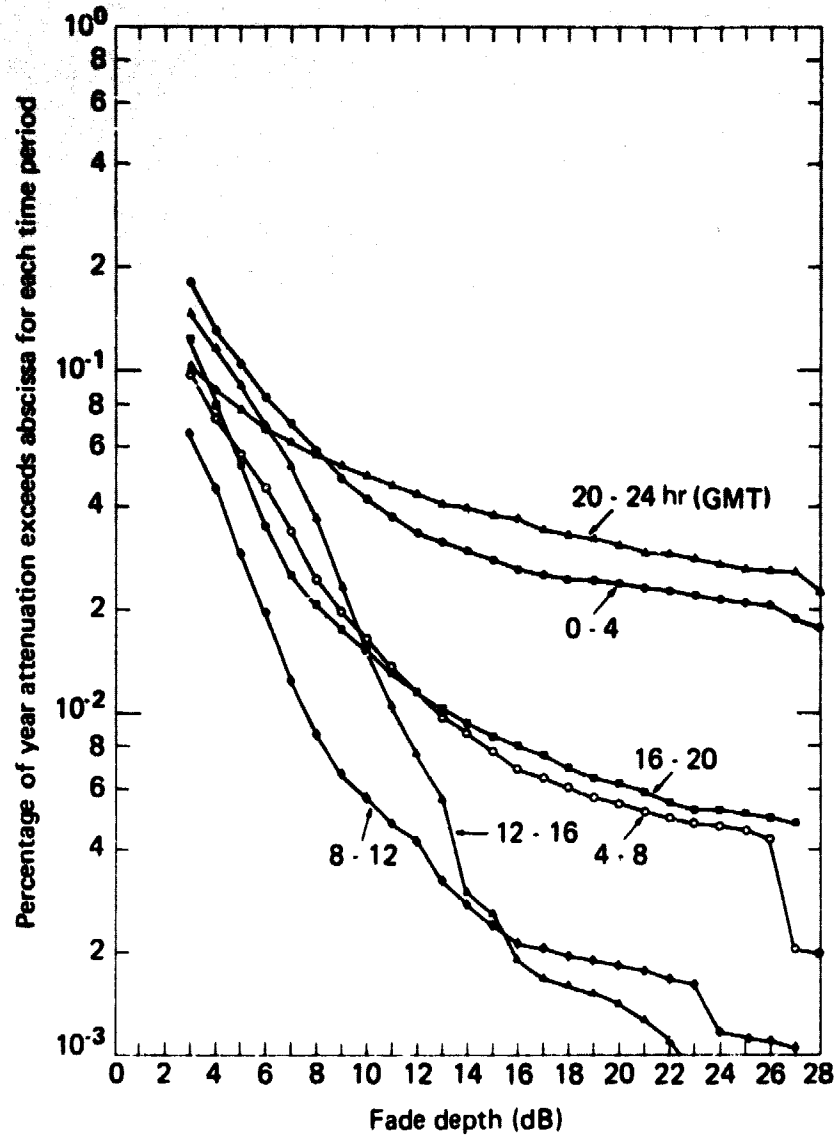

Figure 9. Cumulative distributions for six contiguous four hour time slots (GMT) of the day for the entire year period.

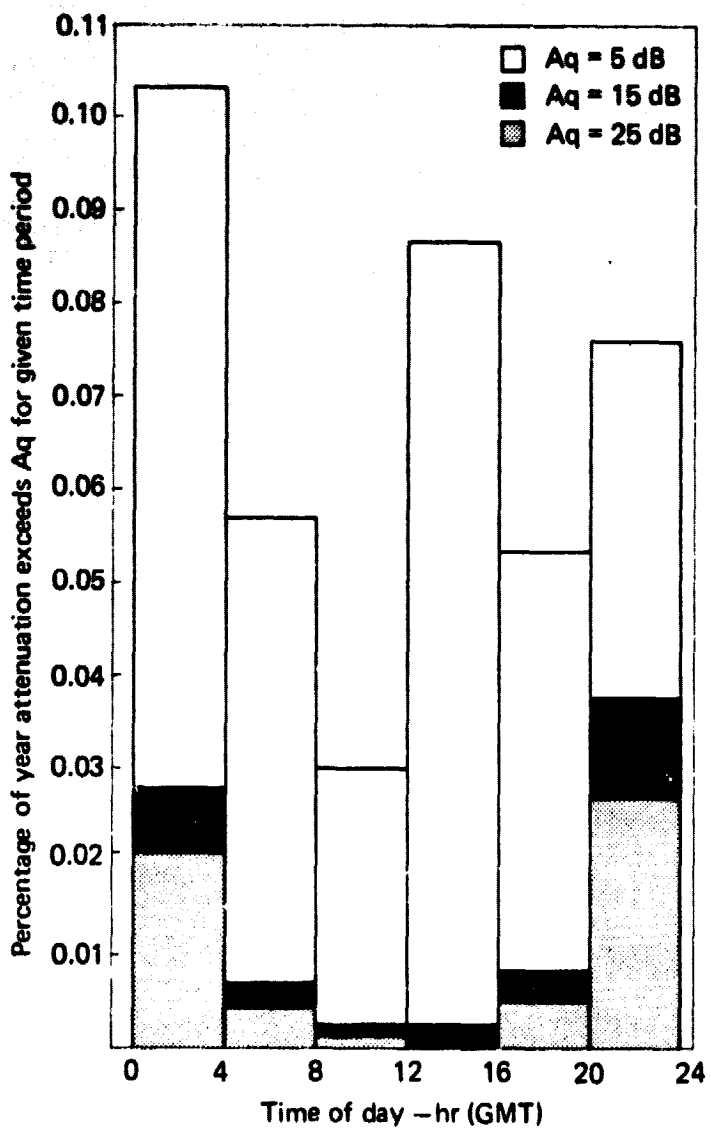

Figure 10. Histogram denoting the percentages of the year the fade depths of 5 (white), 15 (black), and 25 (grey) dB are exceeded for the six contiguous four hour time slots of the day (GMT). Local times are four and five hours less during the summer and winter, respectively.

$$A_{i1} = \alpha_1 R_i^{\beta_1} \ell_{ei} \quad \text{(dB)} \tag{1}$$

$$A_{i2} = \alpha_2 R_i^{\beta_2} \ell_{ei} \quad \text{(dB)} \tag{2}$$

where R_i and ℓ_{ei} are the measured rain rate (mm/hr) and effective path length (km), respectively, at the exceedance probability, P_i, and the parameters, α_1, β_1 and α_2, β_2, are drop size distribution and frequency dependent. These may be calculated using measured or assumed drop size distributions (hereafter referred to as DSD) and the extinction factors of Medhurst [7].

Dividing A_{i2} by A_{i1} we obtain,

$$\frac{A_{i2}}{A_{i1}} = x R_i^{y} \tag{3}$$

where,

$$x = \frac{\alpha_2}{\alpha_1} \tag{4}$$

$$y = \beta_2 - \beta_1 \tag{5}$$

Hence, given a knowledge of the fade distribution at the frequency, f_1, the rain rate distribution and the assumed or calculated parameter values of α_1, α_2, β_1, and β_2, we may arrive at the fade distribution for the frequency, f_2. For example, the fade A_{i2} (at frequency f_2) may be calculated from (3) for the exceedance probability, P_i. The entire distribution at frequency, f_2, may be obtained by repeating the procedure for various exceedance probabilities. This method was employed during the summer of 1977 to obtain the 19.04 GHz distribution from that corresponding to 28.56 (2) and agreement was found to within 0.3 dB rms of the radar measured distribution [4].

We here use Eq. (3) to arrive at the 19.04 GHz fade distribution for the entire year. The values of α and β in Eqs. (4) and (5) are those

calculated using the overall summer data base of disdrometer measurements. These correspond to 460 minutes of disdrometer sampling over 5 rain days.

At a frequency, $f_1 = 28.56$ GHz,

$$\begin{cases} \alpha_1 = 1.76 \times 10^{-1} \\ \beta_1 = 1.021 \end{cases} \tag{6}$$

and at $f_2 = 19.04$ GHz,

$$\begin{cases} \alpha_2 = 7.64 \times 10^{-2} \\ \beta_2 = 1.055 \end{cases} \tag{7}$$

Substituting (6) and (7) into (4) and (5), (3) becomes,

$$\frac{A_i(19.04)}{A_i(28.56)} = 0.434\ R_i^{.034} \tag{8}$$

We note that because β_2 and β_1 are close to unity, their difference is small and the ratio of attenuations as given by (8) is only weakly dependent upon rain rate or exceedance probability.

In Figure 11 is plotted the predicted 19.04 GHz fade distribution (triangle points) using the formulation (8), the 28.56 GHz fade, and the measured rain rate distributions (Figs. 12 and 13), for the year period. The rain rate data was obtained with a nearby tipping bucket raingage and recorded during approximate simultaneous times that fade data were received. Also plotted (circles) in Figure 11 is the predicted 19.04 GHz attenuation deduced from radar derived 28.56 and 19.04 GHz fade distributions and rain rate distributions measured during the summer of 1977 [2,4]. The calculated best fit power ratio obtained from these measurements is,

$$\frac{A_i(19.04)}{A_i(28.56)} = 0.451\ R_o^{.036} \tag{9}$$

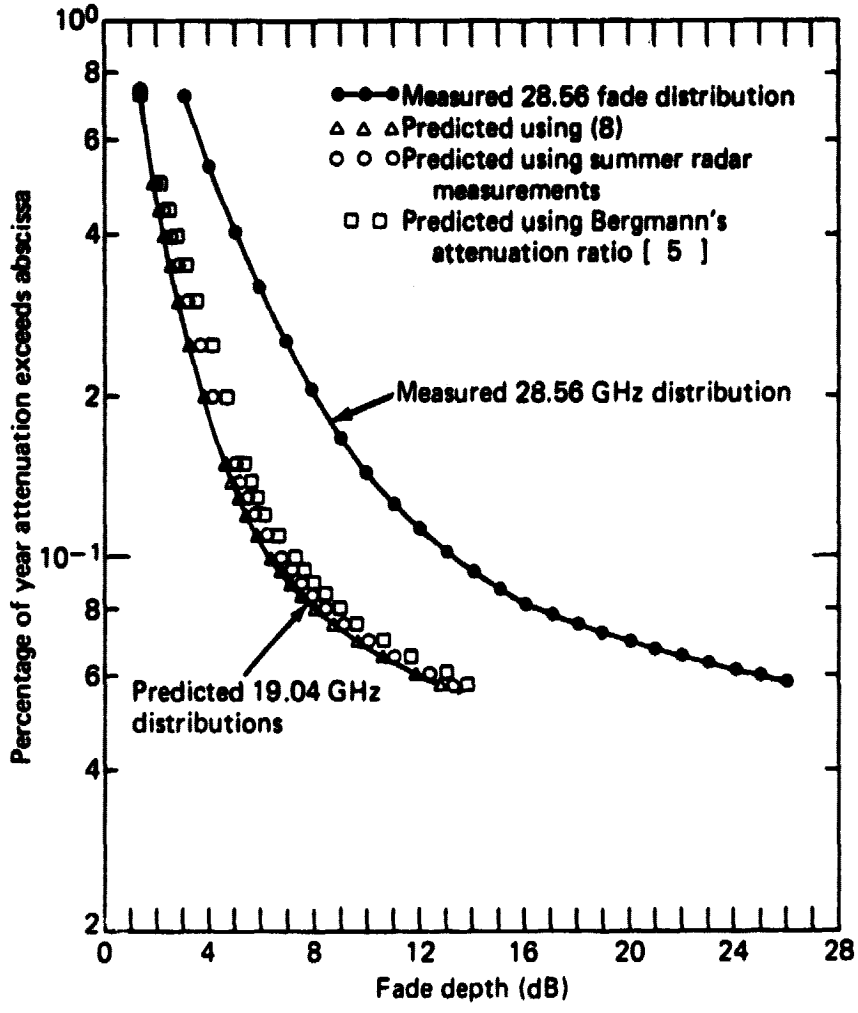

Figure 11. Predicted cumulative fade distributions for the year period for 19.04 GHz.

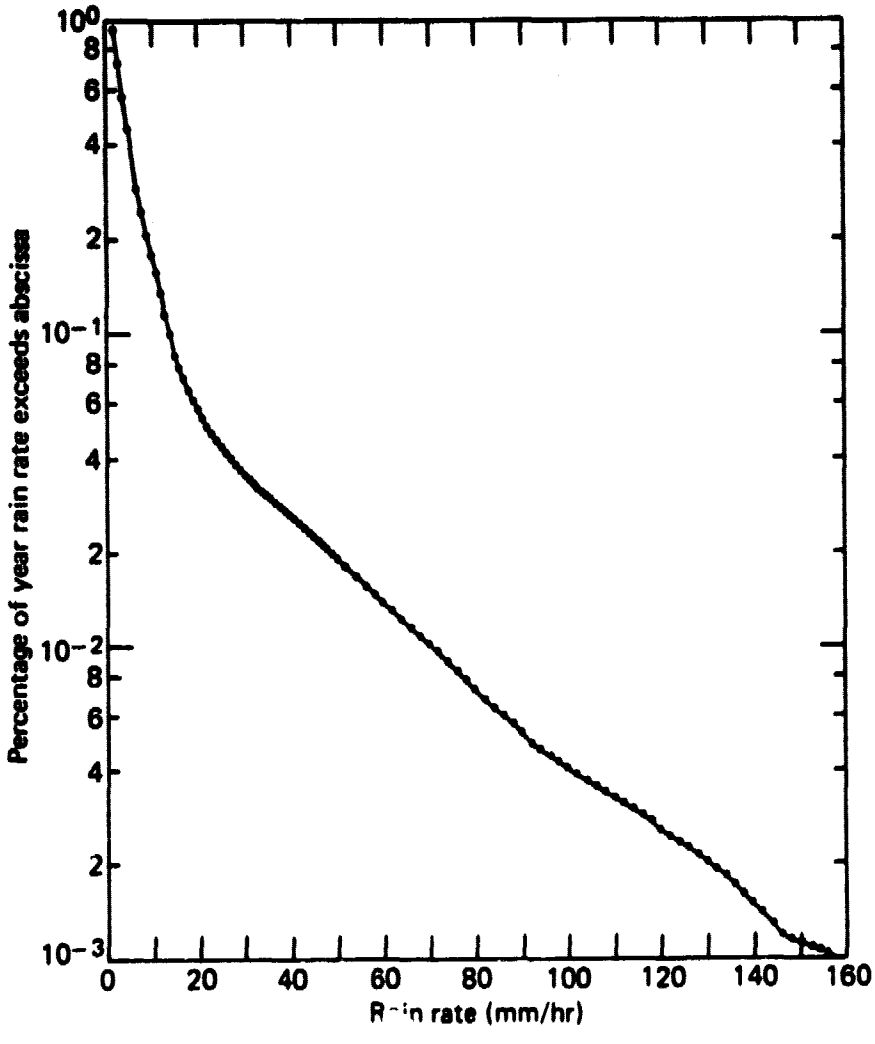

Figure 12. Cumulative rain rate distribution for the year period calculated from raingage data taken during approximate simultaneous times with measured 28.56 GHz fade data (semi-log scale).

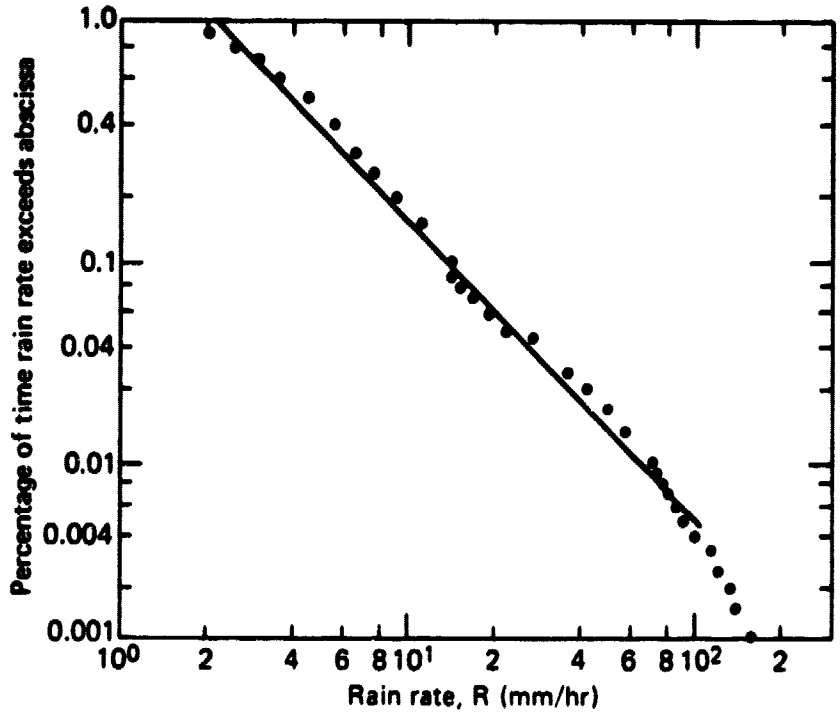

Figure 13. Cumulative rain rate distribution for the year period calculated from raingage data taken during approximate simultaneous times with measured 28.56 GHz fade data (log-normal scale).

Also shown in Figure 11 (squared) is the predicted 19.04 GHz distribution obtained from the average of the attenuation ratios obtained from Bergmann's 28.56 and 19.04 GHz distributions measured at Palmetto, Georgia, from June 1976 to July 1977 [5]. This average was found to be

$$\left[\frac{A_i(19.04)}{A_i(28.56)}\right]_{AVG} = 0.526 \qquad (10)$$

with an associated standard deviation of .014.

By assuming the above ratio to be invariant, the predicted 19.04 GHz distribution for Wallops Island was obtained using the corresponding 28.56 GHz fade distribution. It may be noted that the various predicted 19.04 GHz fades in Figure 11 deviate from one another by, at most, 0.7 dB rms. Close agreement of the attenuation ratio taken from Bergmann's data with that found at Wallops Island does not at all imply a similar DSD but the relative invariance of the attenuation ratio to DSD, at the frequencies considered here, as pointed out in the next section.

4.2 The Approximate Invariance of Attenuation Ratio With Drop Size Distribution

We demonstrate here by theoretical means the approximate invariance of the 19 to 28 GHz attenuation ratio with DSD. The attenuation coefficient may be theoretically expressed by,

$$k = \int_0^\infty C_{ext}(D)N(D)dD \qquad [dB/km] \qquad (11)$$

where $C_{ext}(D)$ [(dB/km) x cm^3] is the extinction factor for a raindrop of diameter, D [cm] and at a propagation frequency, f. Also, $N(D)dD$ [cm^{-3}] is the drop size distribution representing the number of drops between diameters, D and D+dD, per cubic diameter. The extinction factor is a Mie theory related quantity characterizing the attenuation cross section and tabulated in Medhurst [8] as a function of frequency. It may also be approximately expressed by,

$$C_{ext} = C' D^n \qquad (12)$$

where C' and n as a function of frequency may be obtained from the tabulation and plots given by Atlas and Ulbrich [9]. It should be noted that a coefficient C is actually characterized by them, however, because of the difference between our units and theirs, $C' = 4.343 \times 10^5 C$.

As an approximation, we assume the drop size distribution may be represented by,

$$N(D) = N_o \exp(-\Lambda D) \tag{13}$$

where N_o [cm^{-4}] and Λ [cm^{-1}] are arbitrary parameters.

Substituting (12) and (13) into (11) and integrating,

$$k = C' N_o \frac{\Gamma(n+1)}{\Lambda^{n+1}} \tag{14}$$

where $\Gamma(n+1)$ is the gamma function for non-integer arguments. From the plots given by Atlas and Ulbrich [9], we obtain for 19.04 and 28.56 GHz,

$$k_{19} = 5.39 \times 10^6 N_o \frac{\Gamma(5.11)}{\Lambda^{5.11}} \tag{15}$$

$$k_{28} = 7.69 \times 10^6 N_o \frac{\Gamma(4.18)}{\Lambda^{4.18}} \tag{16}$$

and we note that both k_{19} and k_{28} are proportional to N_o and also depend on Λ in approximately the same way. It is therefore apparent that their ratio will have a minimal dependence on drop size distribution. Specifically the ratio of (15) to (16) reduces to,

$$\frac{k_{19}}{k_{28}} = 1.10 \Lambda^{-0.3} \tag{17}$$

As examples, we consider the Marshall-Palmer (hereafter referred to as M-P) distribution [10] and Joss distribution for thunderstorms [11] which have Λ-R (rain rate) relations given by,

$$\Lambda = 41 R^{-0.21} \quad (cm^{-1}) \quad \text{(M-P)} \tag{18}$$

and

$$A = 30\ R^{-0.21} \qquad (cm^{-1}) \qquad \text{(Joss)} \tag{19}$$

where R is in mm/hr. It is interesting to note that although the values of N_o for M-P (.08 cm^{-4}) and Joss (.014 cm^{-4}) are quite dissimilar, these parameters in no way enter into the ratio (17). Substituting (18) and (19) into (17),

$$\left(\frac{k_{19}}{k_{28}}\right)_{M\text{-}P} = .361\ R^{+.062} \tag{20}$$

and

$$\left(\frac{k_{19}}{k_{28}}\right)_{Joss} = .397\ R^{+.062} \tag{21}$$

The ratios (8), (10), (20), and (21) for the various DSD's are depicted in the plots of Figure 14 and we note that they are close in value expecially at rain rates exceeding 10 mm/hr where they are within approximately 20% of one another. These results thus substantiate the contention that the attenuation ratio for the frequencies considered is only weakly dependent on DSD.

It is interesting to note from the results of Atlas and Ulbrich [9], that between f = 20 and 60 GHz, n follows with excellent approximation (coefficient of determination, $r^2 = 0.9992$) the frequency dependence given by

$$n = 4.82 \exp[-8.38 \times 10^{-3} f] \tag{22}$$

where f is given in GHz and where negligible temperature dependence exists between 0 to 40°C. The parameter, C, on the other hand passes through a sharp peak in this interval and has a slight temperature dependence. It is apparent from (14) and (22) that the greater the frequency excursion in the ratio, the greater the dependence on DSD.

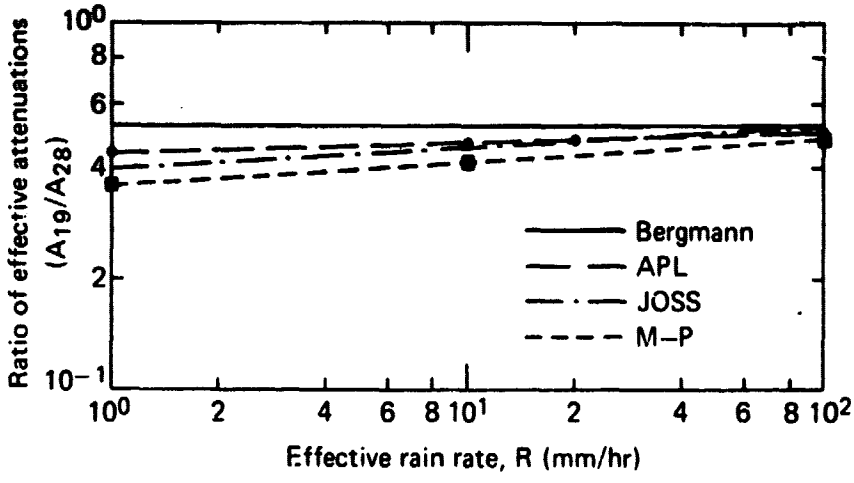

Figure 14. Ratio of 19.04 to 28.56 GHz effective attenuations as a function of rain rate for APL [2,4], Joss [11] and M-P [10] drop size distributions. Also plotted is the average ratio of attenuations obtained from the fade distributions of Bergmann [5].

The relative invariance of the attenuation ratio with DSD at two frequencies (not too widely separated) suggests a useful mechanism for prediction of the fade distributions at a series of other frequencies and at other geographic locations. That is, given a fade distribution at a single frequency as well as a measured rain rate distribution at the same locality, the fade distribution at other frequencies may be determined by use of theoretically derived expressions of the form (20) following methods identical to that described in this section. In the absence of a rain rate measurement, the average ratio of attenuations obtained from measured distributions at one locality may be generally applied at a second locality with small uncertainties of the kind described in this section.

5.0 SUMMARY AND CONCLUSIONS

The results presented here stem from an experimental data base for the climatology of Wallops Island, Virginia, and could be used by the designer of earth-satellite communication systems to establish (a) fade margins, (b) transmitter power and receiver sensitivity requirements, (c) the necessity for space diversity systems, and (d) further predictive methods [12,13]. In the following, we summarize the major results and conclusions of this work.

(1) The cumulative fade and rain rate distributions for the period 1 April 1977 through 31 March 1978 are presented (Figures 2 and 13, respectively) and are shown with good approximation to follow log normal variations over most of the ranges considered. Hence predictive methods of the type described by Lin [6] may, therefore, be employed more conveniently given the ability to describe complex fade distributions analytically.

(2) Attenuations were exceeded for the longest periods of time in August which represented the "worst" month (Figures 3 and 6) for all fades. February was found to represent the "best" month for all fades showing the smallest periods of times that all fade levels were exceeded (Figures 5 and 6). Based on the monthly results, substantially more fade margin would be required for an earth-satellite communication system

for the Wallops Island climatology from May through December than during the balance of the year (Figure 6).

(3) The long term (greater than 25 years) average monthy rainfall data (Figure 7) showed a highest average rainfall month identical to the fade statistics "worst" month (Figure 7). This suggests the possible use of long term rainfall data as an indicator of the worst month for the higher fades.

(4) The eight hour slot of time showing the maximum and minimum number of minutes for which fades exceeded 12 dB are between the hours of 2000 to 0400 GMT (approximately 1600 to 2400 local time) and between 0800 to 1600 GMT (approximately 0400 to 1200 local time), respectively (Figures 9 and 10). These periods represent appropriate time intervals over which satellite transmitter power levels might be enhanced or reduced to compensate for increased or reduced fade periods.

(5) A method is employed using the concept of effective path length applied to the measured 28.56 fade and rain rate distributions to obtain a predicted 19.04 GHz for the year period (Figure 11). This method, which has been previously checked against radar measured distributions [2,4], could be used to predict distributions at other frequencies not too widely separated in frequency.

(6) The ratio of attenuations (not too widely separated in frequency) which are obtained from their distributions at a fixed probability is practically independent of drop size distribution (Figure 14). Hence one may theoretically calculate or measure such a ratio (Section 4) and apply it to the locality in question to arrive at the fade distribution at a second frequency and small uncertainty (e.g., less than 20%). In the absence of rain rate data, one may use the average of the ratio of attenuations for a series of probabilities obtained at one locality to arrive at the fade distribution at the second frequency and at another locality (Figure 11). The influence of different effective path lengths at the various localities does not play a role as the path length cancels out when taking the ratio of attenuations.

6.0 ACKNOWLEDGEMENTS

The author is grateful to John R. Rowland for the development of data processing instrumentation including the disdrometer system. The useful comments and suggestions of Isadore Katz are very much appreicated. Many thanks to Jack Howard and Norman Gebo for assisting in the acquisition of the data at the Radar Atmospheric Research Facility, Wallops Island, Va. This work was performed under contract with NASA/Goddard Space Flight Center (NASA NDPR S50748A; Radar Prediction of Rain Attenuation for Earth-Satellite Paths).

7.0 REFERENCES

1. Cox, D. C., "An Overview of the Bell Laboratories 19- and 28 GHz COMSTAR Beacon Propagation Experiments", The Bell System Tech. J., 57, No. 5, pp 1231-1255, 1978.

2. Goldhirsh, J., "A Demonstration of Methods for Predicting Attenuation Due to Rain Using the 28 GHz COMSTAR Beacon Signal with Radar, Disdrometer, and Raingage Data", Proceedings of the 1978 International Symposium on Antennas and Propagation, Japan, 29-31 August 1978.

3. Goldhirsh, J., "Prediction of Attenuation of the 28 GHz COMSTAR Beacon Signal Using Radar and Measured Raindrop Spectra", Applied Physics Laboratory/The Johns Hopkins University Technical Report, APL/JHU S1R78U-009, 1978.

4. Goldhirsh, J., "Predictive Methods for Rain Attenuation Using Radar and In Situ Measurements Tested Against the 28 GHz COMSTAR Beacon Signal", Applied Physics Laboratory/The Johns Hopkins University Technical Report, APL/JHU S1R78U-010, 1978.

5. Bergmann, H. J., "A MM Wave Propagation Experiment in Georgia and Illinois Utilizing COMSTAR Beacon Signals", 1978 International IEEE/AP-S Symposium, USNC/URSI Spring Meeting, Washington, D. C., 15-19 May 1978.

6. Lin, S. H., "Statistical Behavior of Rain Attenuation", The Bell System Tech. J., 52, No. 4, pp 557-581, April 1973.

7. Crane, R. K. and W. E. Debrunner, "Worst Month Statistics", to be published in Electronic Letters, 1978.

8. Medhurst, R. G., "Rain Attenuation of Centimeter Waves: Comparison of Theory and Measurements", IEEE Trans. Antennas and Propagation, AP-13, pp 550-564, 1975.

9. Atlas, D. and C. W. Ulbrich, "The Physical Basis for Attenuation-Rainfall Relationships and the Measurement of Rainfall Parameters by Combined Attenuation and Radar Methods", Journal De Recherches Atmospheriques, Colloque De L'IUCRM, Vol. VIII, Janvier-Juin, pp 275-298, 1974.

10. Marshall, J. S. and W. McK. Palmer, "The Distribution of Raindrops with Size", J. Meteor., Vol. 5, pp 165-166, 1948.

11. Joss, J., J. C. Thams, and A. Waldvogel, "The Variation of Raindrop Size Distribution in Locarno", Proc. Int. Conf. on Cloud Physics, Toronto, Ontario, Canada, 26-30 August 1967.

12. Goldhirsh, J., "Prediction of Slant Path Rain Attenuation Statistics at Various Locations", Radio Science, Vol. 12, No. 5, pp 741-474, September-October 1977.

13. Goldhirsh, J., "Prediction Methods for Rain Attenuation at Variable Path Angles and Carrier Frequencies Between 13 and 100 GHz", IEEE Trans. on Antennas and Propagation, Vol. AP-23, No. 6, pp 786-791, November 1975.